Non-Diaphragm Shock Tube and Shock Waves in Low Temperature Gases (First report)

Non-Diaphragm Shock Tube and Shock Waves in Low Temperature Gases
(First report)

Kazuo MAENO

Abstract

In the present paper an experimental approach for shock waves and shock-condensation phenomena in low temperature gases (N_2 and R-12) within the limit of $-45°C$ is performed by means of new facilities developed by combining the non-diaphragm (snap-action) shock tube with cooling by liquid nitrogen. Together with the measurements for temprature, incident and reflected velocities of the wave, and pressure history, the experiment of flow visualization is conducted, which shows wall condensation phenomenon of R-12 behind the reflected shock wave.

1. INTRODUCTION

Shock tube is one of the prominent apparatuses for the experiments on high speed gasdynamics. Conventional types of shock tube, however, have the problems of contamination and atmospheric influx or freezing of water vapor during the exchange of broken diaphragms, so they were not utilized to the experiments for the gas below room temperature without complicated contrivance for the diaphram exchange.[1),2)] This is the reason why many investigations have been restricted to the gases which were initially in room temperature or in high temperature range.

Recently the necessity of fluid dynamical approaches to such applicative engineering as coolant recurrence, LNG transportation, and cryogenic superfluid technology has developed enough. Especially dynamics of multiphase flow or high speed gasdynamics for fluids from room temperature to cryogenic range have been of great interest. Practical data, however, for these fields are quite inadequate.

In this paper the new apparatus for shock experiments in low temperature fluid is contrived, which unites the non-diaphragm shock tube[3),4)] with cooling by liquid nitrogen. Making use of the apparatus, fundamental parameters, e.g. shock velocities and pressure history, of test gas N_2 or R-12 (Freon 12; CCl_2F_2, dichlorodifluoromethane) are measured to investigate the behavior of shock waves in low temperature gases. Furthermore the possibility of condensation behind the shock wave in R-12 is checked up.

2. EXPERIMENTAL SETUP

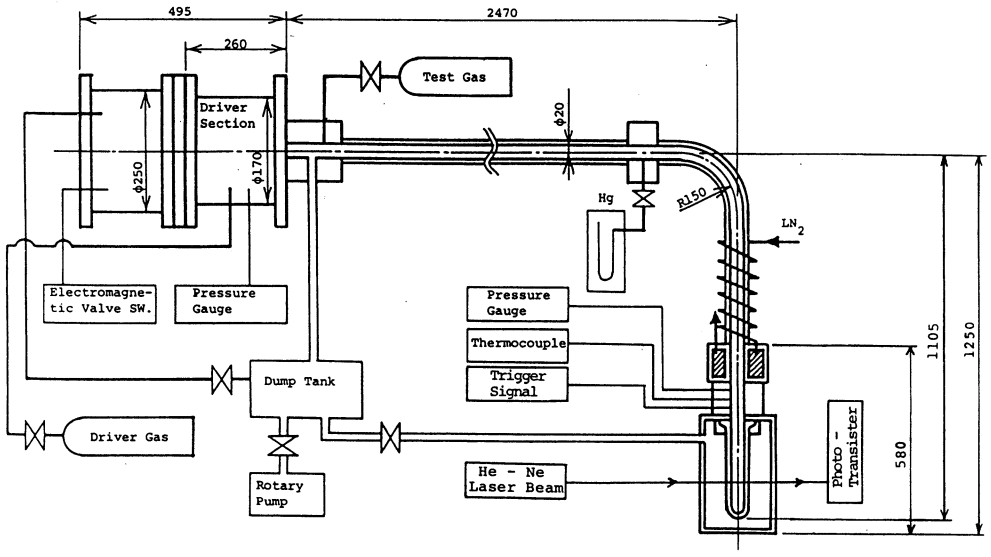

Fig. 1 Experimental setup

The schematic diagram of shock tube apparatus is shown in Fig.1. The outlooks of high-pressure driver chamber and test section are also represented in Fig. 2 -(a) and 2 -(b), together with the mechanical assembly of driver section in Fig. 2 -(c). Non-diaphragm (snap-action) shock tube newly devised has a main piston made of nylon, which is substituted for conventional diaphragm, and also has an auxiliary nylon piston controlled by an electromagnetic valve for rapid release of rearward high pressure gas. The basic mechanism of this driver section is similar to those reported in Refs. 3) and 4). The volume of high pressure driver is 2700cm^3, and maximum usable pressure is about 500 KPa. Nitrogen is employed as a driver gas, and the pressure in driver chamber is monitored by semiconductor pressure transducer (TOYODA; PMS-5 H). Behind the high pressure chamber, evacuative section around the valve is settled to move both pistons rearward promptly, and to prohibit from air regurgitating. On account of the driver mechanism, this shock tube is free from pollution by broken diaphragm or freezing influx of atmosphere, and many cryogenic operations are possible with retaining the low pressure chamber in low temperature by liquid nitrogen.

For the driven section, seamless stainless tube of 19.4mm inner diameter is utilized, whose horizontal and straight length is 2.3m. In order to maintain the constant cold conditions or saturation phase equilibrium, the low pressure tube has 90° bend portion of curvature radius 150mm after the

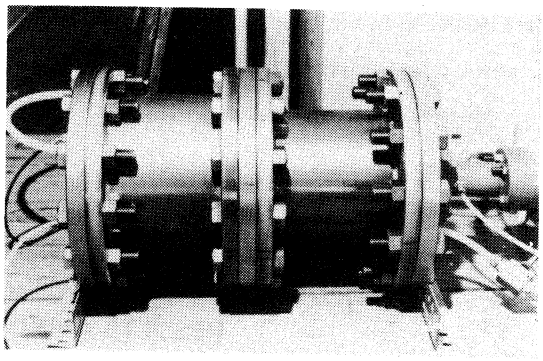

(a)

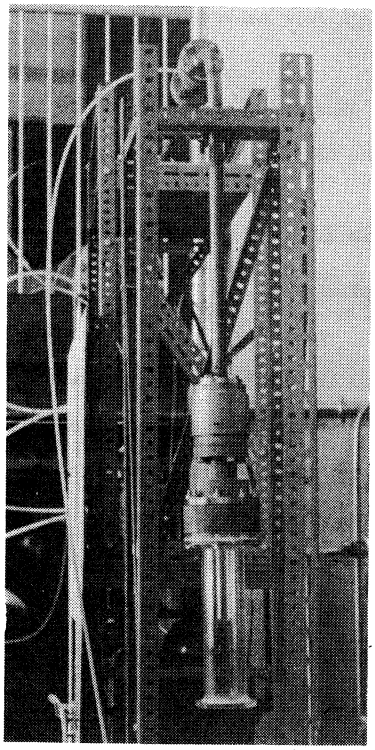

(b)

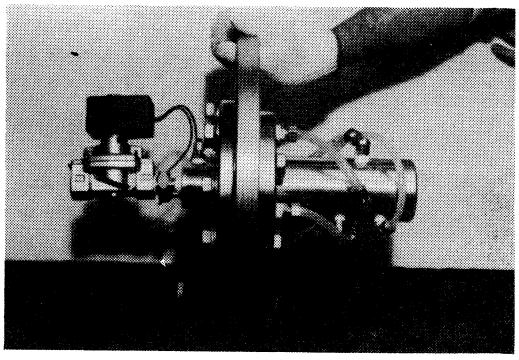

(c)

Fig. 2 Photographs of experimental apparatus

straight part, and has also vertical section of about 1m length. The diffraction and disturbances of shock wave passing through this bend portion are not considered to be so strong in the vertical downstream region of several times as long as the tube diameter, because the ratio of curvature radius of the bend to tube radius is the order of 15.[5] Cooling section with liquid nitrogen, and vacuum heat shield chamber are also equipped to the vertical tube. The end part of vertical tube is a glass cylinder of 220mm length for flow visualization or He-Ne laser beam transparency.

The velocities of incident and reflected shock waves are measured from duration between the trigger signal by a lead zirconate-titanic solid-solution piezoelectric pressure element (Tokin; NPM-ND 5^{Φ}) and the steep rise of electrical signal from phototransistor (TPS-603) by passing of the wave front through He-Ne laser beam. Pressure variation behind the shock is monitored by semiconductor pressure transducer (TOYODA; PMS-50H) in room temperature gas, and sup-

plemental pressure monitor by the piezoelectric element (AC signal) is conducted in low temperature environment. Initial temperature of the gas in test section is measured by CA thermocouple. Measured data are amplified to be recorded by a storage oscilloscope (Kikusui; DSS-6521). They can be processed by micromputer (NEC; PC-8801) by way of A-D converter (Microscience; DAS-1280 BPC).

The driver section is roughly isolated thermally by multilayer heat shield of aluminium foil and vinyl sheet, and partly by polymer form, together with the vacuum shield chamber.

3. RESULTS AND DISCUSSION

3—1. Fundamental Characteristics of Shock Waves

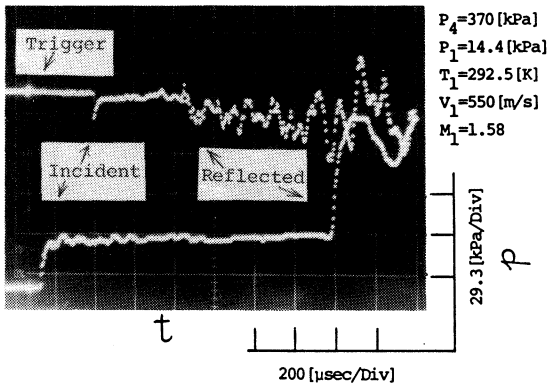

Fig. 3 Shock pressure signal and phototransistor signal by He-Ne laser beam for room temperature N_2

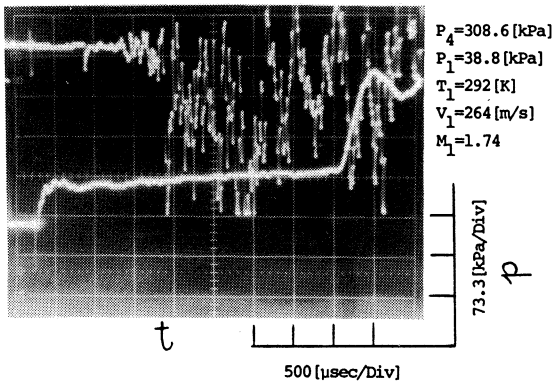

Fig. 4 Shock pressure and phototransistor signals for R-12 test gas in room temperature

As for the test gas N_2 in room temperature T_1, measured data are presented in Fig. 3, where p_4 is driver pressure, p_1 is the initial pressure of test gas, v_1 is incident shock velocity, and M_1 denotes incident shock Mach number. Pressure variation behind the incident and reflected shock waves is the lower trace, and signal from phototransistor by He-Ne laser beam deffraction is the upper trace. Rapid pressure increase by the arrival of incident/reflected shock wave and steep variation of phototransistor signal by laser beam diffraction from the passage of wave front are observed. Disturbed laser signal after shock reflection is considered to originate from the interaction of reflected shock wave with boundary layer behind the incident shock.

Figure 4 indicates the measured data for test gas of room temperature R-12 (specific heat ratio; $\gamma = 1.14$, sound velocity; a $= 152$m/s, molecular weight; 120.9, atmospheric boiling point; 243.5K).[6] Compared with the results in Fig. 3,

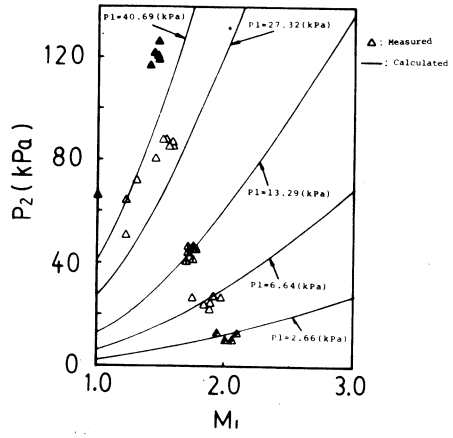

Fig. 5 Pressure p_2 behind the shock wave to incident shock Mach number M_1 for test gas N_2

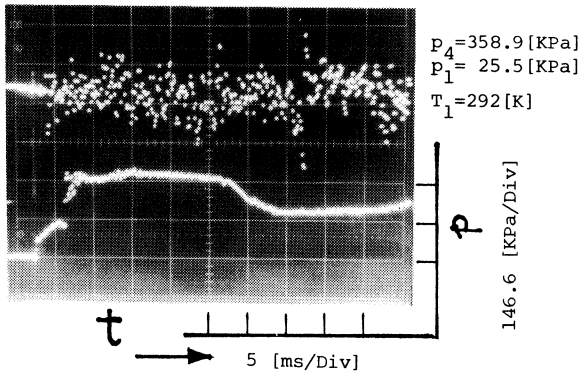

Fig. 6 Shock pressure and phototransister signals for R-12 in room temperature (long time range)

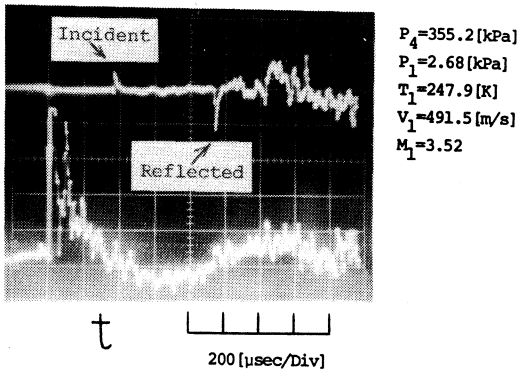

Fig. 7 Phototransistor signal and NPM piezoelectric pressure element signal for the shock wave in low temperature R-12

it is remarked that the diffraction signal of laser beam behind the shock reflection shows much more furious disturbances. This phenomenon occurs from the stronger interaction between the reflected shock and boundary layer behind the incident shock wave, as the specific heat ratio of R-12 is far smaller than N_2. Moreover, the condensation at the tube wall after the reflected shock[7] and the condensed droplets behind shock wave also have strong effect on this phenomenon to scatter the laser beam. Practically laser beam scattering by very small condensed droplets can be visible after the arrivals of reflected shock wave or contact surface.

Gradual increase of the pressure behind incident shock seems to be originated by energy relaxation of R-12 molecules with the high degree of intramolecular freedom. The measured pressure p_2 behind the incident wave from the photographs can be compared with the results calculated from initial conditions and measured shock velocity by Rankine-Hugoniot relations with constant specific heat ratio. The compared data represent favorable coincidence for test gas N_2 as shown in Fig. 5 , while measured p_2 for R-12 shows lower distribution than estimated results, which is also due to molecular relaxation effects. Figure 6 indi-

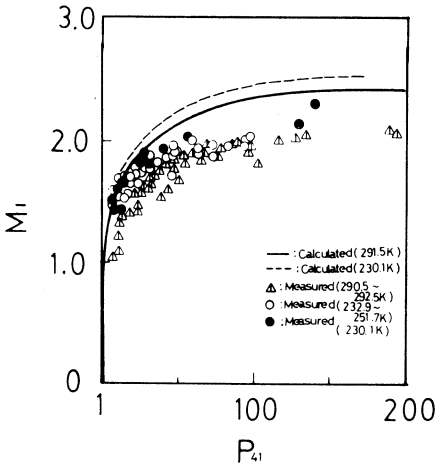

Fig. 8 Incident shock Mach number M_1 and pressure ratio p_{41} for N_2

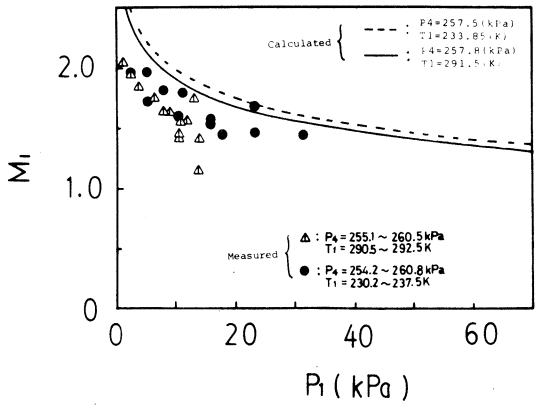

Fig. 9 Incident Mach M_1 and initial pressure p_1 of N_2 for fixed driver pressure p_4 of N_2

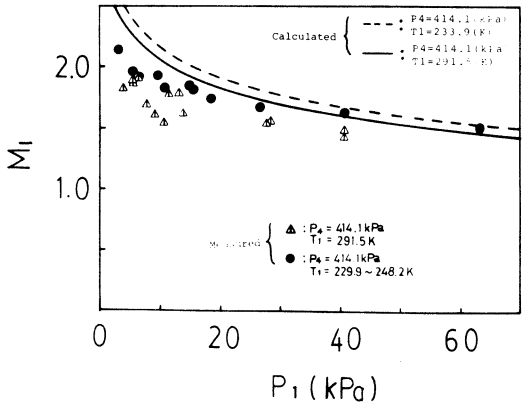

Fig. 10 Similar relation between M_1 and p_1 to Fig. 8 for another fixed p_4

cates the data in long time range for room temperature R-12, from which it can be seen that the stagnant conditions behind reflected shock wave are maintained for about 20ms after reflection.

As the typical result for test gas R-12 in low temperature, Fig. 7 shows the trigger signal from piezoelectric pressure element (NPM-ND 5^{Φ}) in lower trace and phototransistor signal in upper trace. This is an example of low initial pressure p_1, so the condensation effect cannot be confirmed clearly.

Figure 8 represents the relation between incident shock Mach number M_1 and pressure ratio p_{41} of driver gas N_2 to test gas N_2. Solid line is the calculation curve for an ideal and onedimensional shock tube in room temperature. Dashed line shows the calculated curve for low temperature N_2, and the difference between sound velocities of room and low temperature results in higher distribution. Measured data for our non-diaphragm shock tube indicate lower distributions than the calculation curves, and including some errors, measured incident Mach M_1 for low temperature N_2 shows higher trend than the measurement for room temperature N_2. This tendency appears also in Fig. 9 and Fig. 10 which express the relations between the incident shock Mach number M_1 and initial

pressure p_1 of N_2. As shown in these figures, stronger incident shock wave can be obtained from the lower initial temperature range.

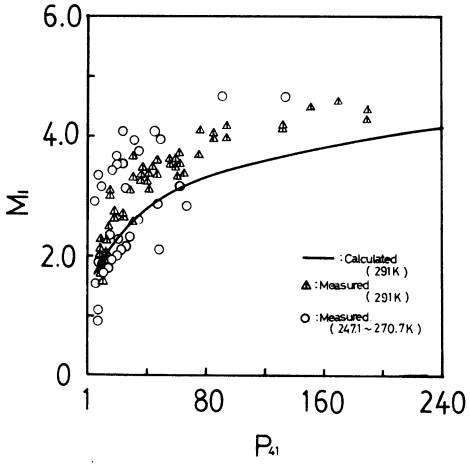

Fig. 11 Incident shock Mach number M_1 and pressure ratio p_{41} for R-12

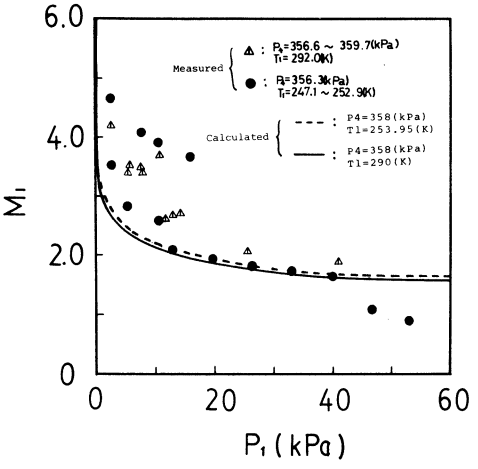

Fig. 12 Incident Mach M_1 and initial pressure p_1 of R-12 for fixed driver pressure p_4 of N_2

In all cases shown above, it is clarified that the repetitive operations of our shock tube apparatus in low temperature range to the degree of $-45°C$ have no problems.

Figure 11 indicates the relation between M_1 and p_{41} for test gas R-12. Solid line is the calculated results for ideal shock tube, and owing to the little difference of sound velocities, estimated curves for room and low temperature coincide with each other. In general, measured M_1 distributes higher than calculation curve in this experiment. As the nonequilibrium condensation behind shock wave is likely considered to diminish the shock strength, the results in Fig. 11 show some contradiction. In this figure there can be seen two different tendencies for low temperature R-12. This result appears also in Fig. 12 which represents incident Mach distribution to pressure p_1 of R-12 for fixed p_4 of N_2. Since some error in the measurement may be infered, more precise experiments about this combination of conditions are necessary, including the reliability check of CA thermocouple and cooled conditions in test section. Figure 13 shows the similar relations to Fig. 12 of R-12 for different driver pressure p_4 of N_2. In these figures, calculated curves are obtained from variable specific heat ratio γ with respect to temperature T given by

$$\gamma = 1.169 + 8.2 \times 10^{-6} (T - 220)^2,$$

for the saturation vapor of R-12.

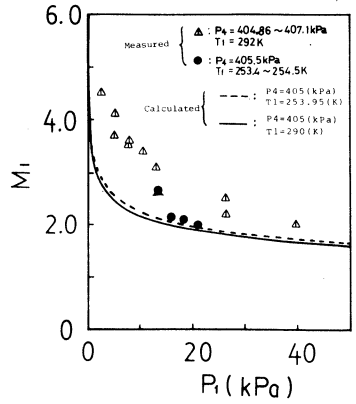

Fig. 13 Similar relation between M_1 and p_1 to Fig. 11 for another fixed p_4

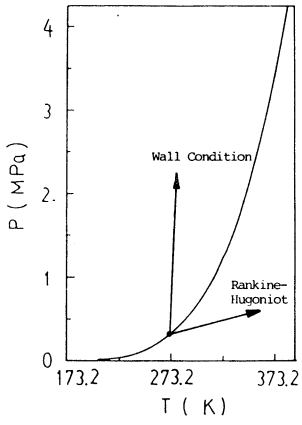

Fig. 14 Equilibrium saturation curve of R-12

3 — 2. Flow Visualization

In our experiment, if the test section is cooled enough by liquid nitrogen below the equilibrium boiling point of R-12 under a given pressure p_1, condensed liquid phase accumulates at the bottom of cylindrical glass end of the vertical tube to accomplish liquid-gas phase equilibrium in test section. The saturation curve of R-12 is presented in Fig. 14. If the incident or reflected shock wave progresses into the gas in such phase equilibrium, flow parameters, p and T, behind the shock jump up to the right hand direction according to Rankine-Hugoniot relations as shown in Fig. 14. The temperature of the gas closely adjacent to the wall, however, cannot follow the jump condition, and condensation effect[8),9)] may play an predominant role at solid wall or liquid surface[7)].

As a matter of course, such molecules of high molecular weight as R-12 have many intricate degrees of intramolecular freedom, so the different kind of energy relaxations are accompanied with the shock jump. Consequently the explanation for such shock wave as in Freon in equilibrium dose depend on the development of further detailed researches in the aspects of real gas effect.

Figure 15 represents motor-driven photographs of the behavior of liquid-gas R-12 phase interface before [(a)] and after [(b)—(f)] shock reflection. Since the frame speed is slow (maximum speed; 5 frames/sec), incident and reflected wave fronts cannot be snapshotted. But the first disturbance of interface by shock reflection or contact surface arrival can be recognized [(b)], along with the far later disturbance by boiling of liquid phase [(f)]. Condensed liquid film on vertical wall can also be seen in the photograph [(b)].

The high-speed shadowgraphs of the liquid-gas interface are shown in Fig. 16(a)—(h). These shadowgraphs are taken by high speed camera (Osawa; HYCAM 40 — 0004) with the frame speed of 1480 frames/sec. It can be seen from these figures that the condensation layer on glass tube wall begins to climb up after shock reflection [(a)], though the reflected shock cannot be recorded. After clambering the adiabatic glass wall up to the order of cylinder radius, the condensation layer

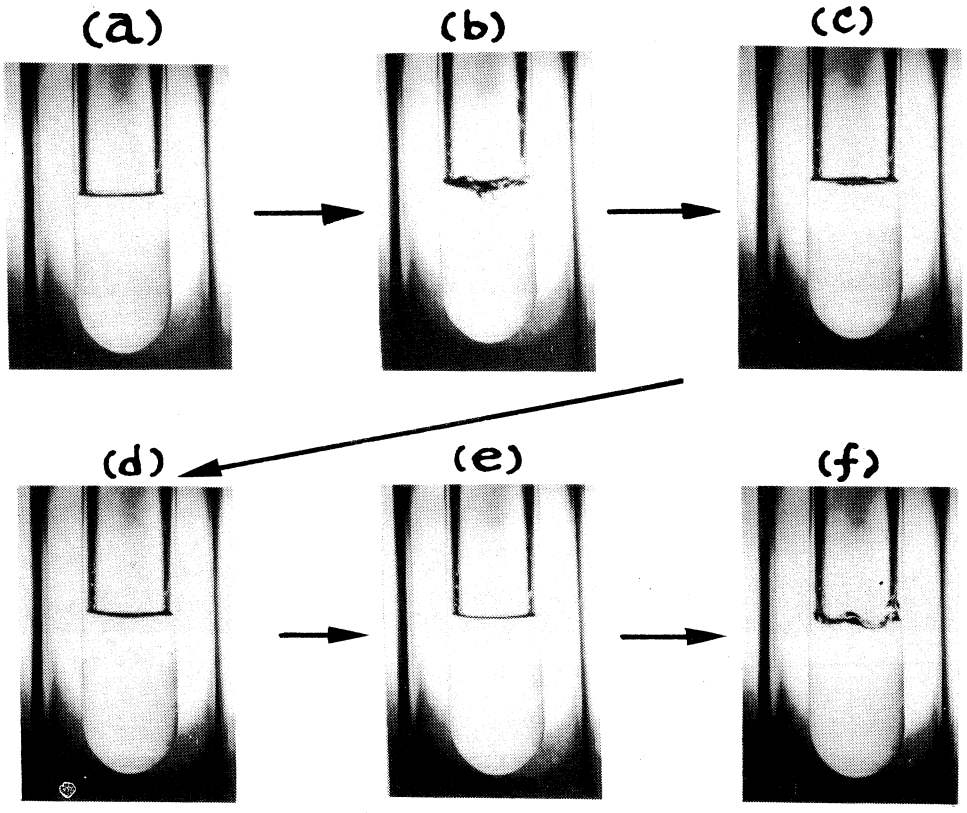

T_1 = 248.3K, p_1 = 13.3KPa
T_4 = 288.7K, p_4 = 521.6KPa
Exposure; 32, Shutter speed; 1/250
400ms/frame

Fig. 15 Photographs of liquid-gas interface taken by motor-driven camera [(a); before shock incidence, (b) - (f); after shock reflection]

starts to vaporize slowly in the stagnant circumstances behind shock reflection and contact surface interaction [(c)—(d)]. Some degree of disturbances or vaporizing instability can be observed in Fig. 16(e)—(h). The photographs shown in Fig. 16 clealy corroborate the condensation phenomenon at cold tube wall behind the reflected shock wave in low temperature R-12. It can be also remarked that in our experiment the condensation after shock reflection begins to proceed from liquid-gas interface up to the stagnant tube wall.

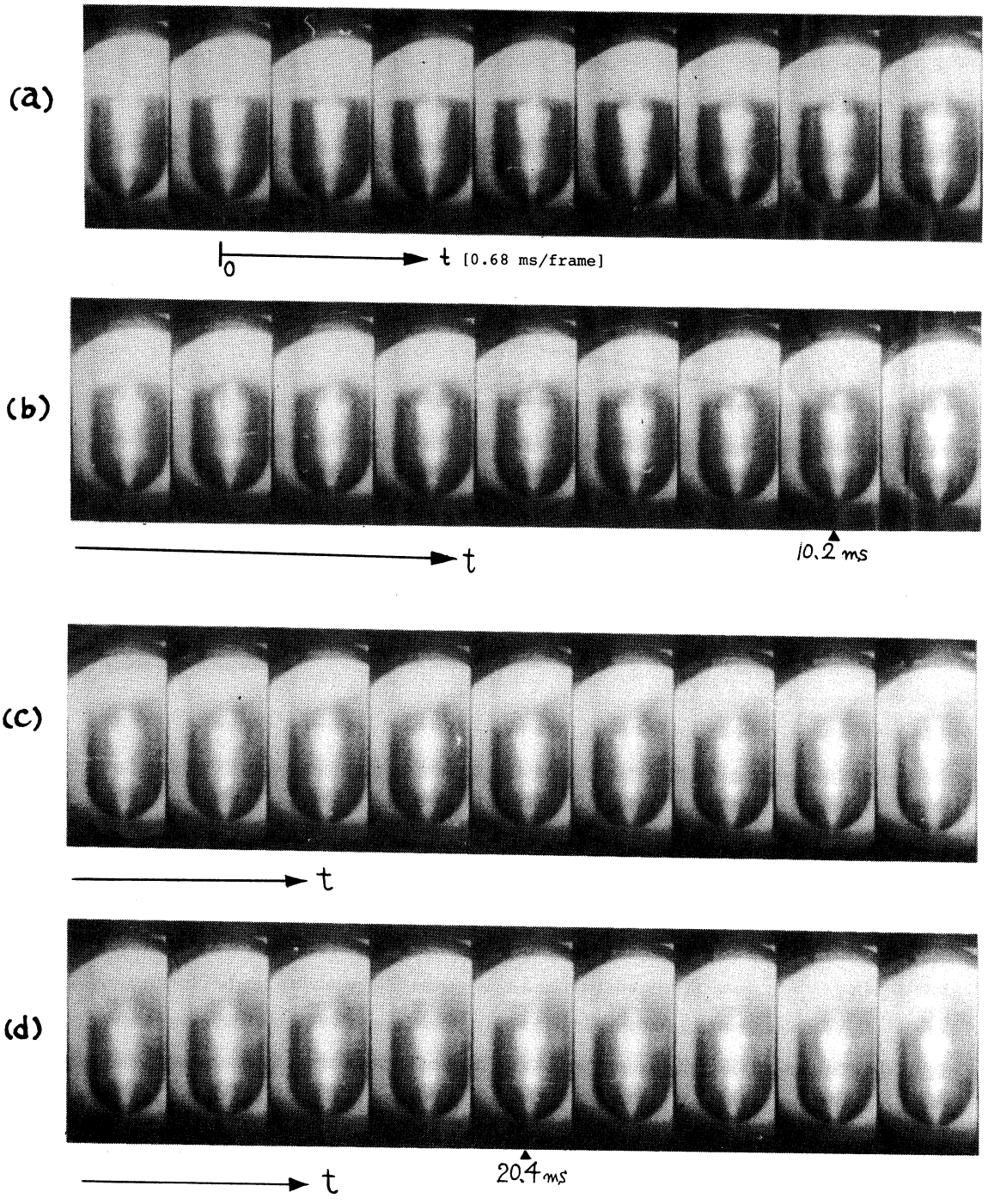

Fig. 16 Shadowgraphs of the behavior of R-12 liquid-gas interface taken by high-speed camera (1480frames/se
p_1 =40KPa, T_1 =255.6K, p_4 =520KPa

(e)

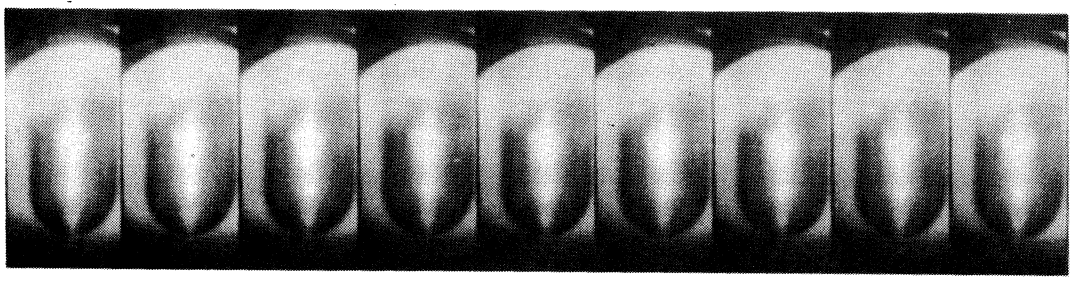

t

(f)

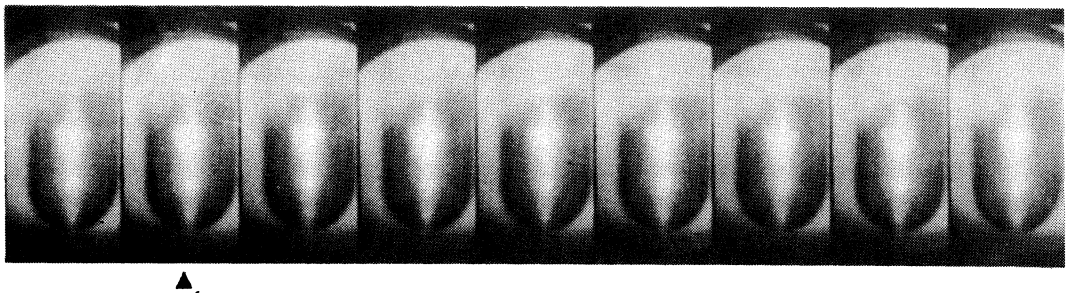

30.6ms

t

(g)

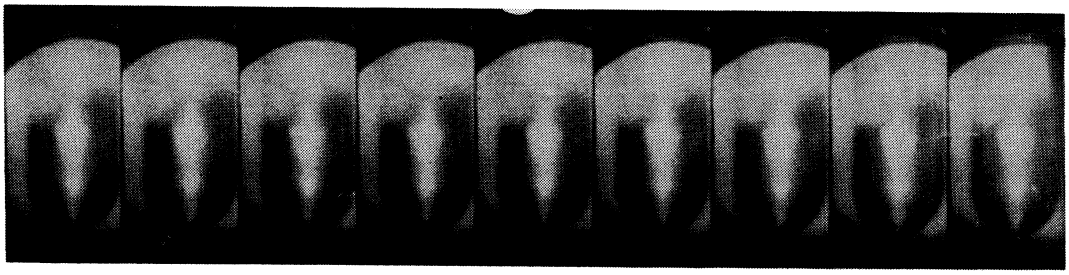

t

40.8ms

(h)

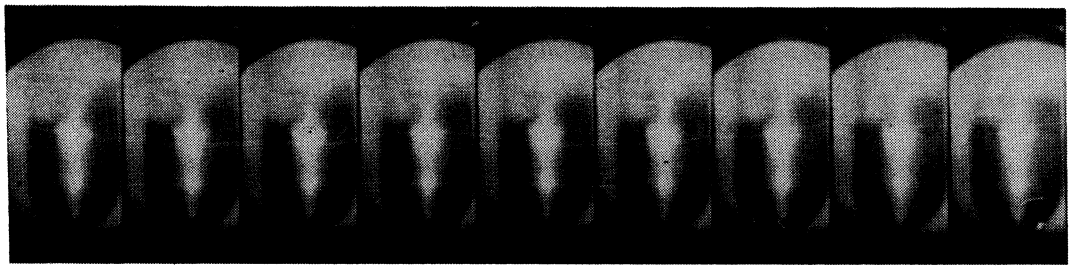

t

4. CONCLUDING REMARKS

A new apparatus of shock wave experiment in low temperature gases is contrived by assorting the non-diaphragm (snap-action) shock tube with cooling by liquid nitrogen. Measurements are performed for shock waves in N_2 and R-12 of temperature range from room conditions to the degree of $-45°C$, and fundamental shock wave paramenters are obtained. The operations of our shock tube in such low temperature range present no problems. Complicated real gas effects on shock behavior of R-12 are observed. Among other results obtained, a strong condensation phenomenon at the tube end wall behind the reflected shock wave in low temperature R-12 is corroborated to exist from laser beam scattering and flow visualization by high speed shadowgraphs.

(Received May 21, 1985)

ACKNOWLEDGMENT

The author is grateful to express his sincere thanks to Prof. Y. Hanaoka of Muroran Institute of Technology for his continual encouragement and to Mr. A. Yamazaki for his experimental support, and also to Mr. S. Orikasa of Nissan Motor Co., Ltd. for his endeavored experiments for Master Thesis and valuable discussion.

REFERENCES

1) H. W. Liepmann, J. C. Cummings, and V. C. Rupert; "Cryogenic Shock Tube," The Phys. of Fluids, Vol. 16, No. 2 (1973), pp. 332−333.

2) J. C. Cummings; "Experimental Investigation of Shock Waves in Liquid Helium I and II," J. Fluid Mech., Vol. 75, Part 2 (1976), pp. 373−383.

3) H. Oguchi, K. Funabiki, S. Sato, and K. Maeno; "An Experimental Study on CO_2 Gasdynamic Laser by Means of Non-Diaphragm Shock Tubes," Bulletin of ISAS (in Japanese), Vol. 14, No. 2 (B) (1978), pp. 809−829.

4) K. Maeno, K. Funabiki, and H. Oguchi; "Experimental and Analytical Study of CO_2/N_2 Mixing Gasdynamic Laser," ISAS Report (No. 593), Vol. 46, No. 5 (1981), pp. 175−197.

5) K. Takayama and O. Onodera; "Shock Wave Propagation Past Circular Cross Sectional 90° Bends," Shock Tubes and Waves (Proc. 14th Int. Symp. on Shock Tubes and Shock Waves), Ed. by R. D. Archer and B. E. Milton (1983), pp. 205−212.

6) N. B. Vargaftik; "Thermophysical Properftes of Gases and Liquids," Nauka (USSR) [translated in Japanese (1974), pp. 369−372].

7) S. Fujikawa and T. Akamatsu; "Effects of The Non-Equilibrium Condensation of Vapour on The Pressure Wave Produced by The Collapse of A Bubble in A Liquid," J. Fluid Mech., Vol. 97, Part 3 (1980), pp. 481−512.

8) G. Dettleff, P. A. Thompson, G. E. A. Meier, and H. Speckmann; "An Experimental Study of Liquefaction Shock Waves," J. Fluid Mech., Vol. 95, Part 2 (1979), pp. 279−304.

9) P. A. Thompson and D. A. Sullivan; "On The Possibility of Complete Condensation Shock Waves in Retrograde Fluids," J. Fluid Mech., Vol. 70, Part 4 (1975), pp. 639−649.